Electrocatalytic reduction of CO2 and nitrate on immobilized metal porphyrins

Shen, Jing

Citation
Shen, J. (2015, December 9). *Electrocatalytic reduction of CO2 and nitrate on immobilized metal porphyrins*. Retrieved from https://hdl.handle.net/1887/36535

Version:	Corrected Publisher's Version
License:	Licence agreement concerning inclusion of doctoral thesis in the Institutional Repository of the University of Leiden
Downloaded from:	https://hdl.handle.net/1887/36535

Note: To cite this publication please use the final published version (if applicable).

Cover Page

Universiteit Leiden

The handle http://hdl.handle.net/1887/36535 holds various files of this Leiden University dissertation

Author: Jing Shen
Title: Electrocatalytic reduction of CO2 and nitrate on immobilized metal porphyrins
Issue Date: 2015-12-09

Chapter 4

Electrocatalytic Nitrate Reduction by a Cobalt Protoporphyrin Immobilized on a Pyrolytic Graphite Electrode

ABSTRACT

A series of simple molecular catalysts, i.e. Cobalt (III), Iron (II), Nickel (II), Copper (II) and Rhodium (II) protoporphyrins (metal-PP), directly adsorbed on pyrolytic graphite, has been utilized for catalyzing the electrochemical reduction of nitrate. These catalysts are studied by combining cyclic voltammetry with online electrochemical mass spectrometry (OLEMS), to monitor volatile products, and online ion chromatography (IC), to detect ionic products in the aqueous electrolyte solution. Among all investigated porphyrins, the Co-based protoporphyrin shows highest selectivity towards hydroxylamine (NH_2OH), which made it the catalyst of primary interest in the paper. The reactivity and selectivity of the immobilized Co-protoporphyrin depends significantly on pH, more acidic conditions leading to higher reactivity and higher selectivity towards hydroxylamine over ammonia. Potential controlled electrolysis results show that the potential also greatly influences the selectivity: at pH 1, hydroxylamine is the main product around -0.5 V with approximately 100% selectivity, while hydroxylamine and ammonia are both formed at more negative potential, -0.75 V. The mechanism of the reaction is discussed, invoking of the possibility of two pathways for hydroxylamine/ammonia formation: a sequential pathway, in which hydroxylamine is produced as an intermediate, with ammonia subsequently formed through reduction of NH_2OH/NH_3OH^+; and a parallel pathway, in which the formation of hydroxylamine and ammonia derives from a common intermediate.

The contents of this chapter has been published in: Jing Shen, Yuvraj Y. Birdja and Marc T.M. Koper. Langmuir, **2015**, 31 (30), pp 8495–8501.

4.1. Introduction

The extensive use of ammonium nitrate as a fertilizer makes nitrate a major source of contamination in ground and drinking water. An excess of nitrate in drinking water can cause shortness of breath and blue baby syndrome[1-3]. The electrochemical reduction of nitrate would be a possible way to remove nitrate, provided it would convert nitrate in water to dinitrogen, which is harmless to the environment[4]. Nitrate reduction may also produce valuable chemicals like hydroxylamine, which is an important raw material for the chemical industry[5,6]. However a large number of stable products can be generated from electrochemical nitrate reduction: NO_2, NO_2^-, HNO_2, NO, N_2O, N_2, NH_2OH and NH_3, which makes selectivity a critical issue[7-10].

Metalloporphyrins and various other metal complexes have been employed as catalyst for the electrochemical reduction of nitrate, nitrite and nitric oxide. Iron porphyrin nitrosyls, FeP(NO), where P = TPP (tetraphenylporphyrin), TPC (tetraphenylchlorin), or OEP (octaethylporphyrin), were reduced in nonaqueous solvents to give hydroxylamine and ammonia as products[11]. In aqueous solution, the reduction of nitrite to ammonia has been shown to be catalyzed by FeTSPP (dianion of tetrakis(4-sulfonatophenyl) porphyrin)[12], and a water-soluble cobalt porphrin, Co(2-TMPyP) (tetrakis (N-methyl-2-pyridyl) porphine) was utilized for the electrochemical reduction of nitric oxide to hydroxylamine and ammonia[13]. Taniguchi et al. explored the ability of metal cyclams, Cobalt (III) and Nickel (II) cyclam (cyclam = 1,4,8,11-tetra-azacyclotetradecane), to electrocatalyze nitrate reduction on mercury electrode, giving hydroxylamine as main product. They also speculated that the effective catalyst was probably an adsorbed Co^I or Ni^I cyclam species[14, 15]. Later, these cyclams were immobilized on the surface of a gold electrode by incorporating them into a Nafion film, by direct adsorption or by linking to pyrrole and subsequent eletropolymerization, to catalyze nitrate reduction in alkaline solution[16-19]. A metal phthalocyanine modified on a glassy carbon electrode has also been shown to have activity for the nitrate reduction in alkaline media to give ammonia as the main product[20, 21]. Furthermore, a Mo-Fe cluster modified electrode[22], heteropolyanions containing tungsten, molybdenum, Copper (II) or Nickel(II),[23] and multicopper-containing

hetero-polyoxotungstates[24] have all been found to be active for the electrochemical reduction of nitrate.

Iron-protoporphyrin modified pyrolytic graphite electrodes have previously been shown to be very selective catalysts for the reduction of nitric oxide and nitrite in acidic media[25, 26]. Building on these previous results from our group, in this work, a simple metal-containing complex, cobalt protoporphyrin (CoPP), directly adsorbed on pyrolytic graphite (PG) electrode, was utilized as an electrocatalyst for the reduction of nitrate in acidic solution. CoPP was chosen among a series of metal-PPs because it has the highest reactivity and selectivity toward hydroxylamine. The electrochemical nitrate reduction was investigated by combining online electrochemical mass spectrometry (OLEMS) and ion chromatography (IC) with cyclic voltammetry. We find that pH and potential play a significant role in both reactivity and selectivity. A possible mechanism will also be discussed.

4.2. Experimental Details

4.2.1. Chemicals

Cobalt (III) protoporphyrin IX chloride (Frontier Science), Iron (II) protoporphyrin IX chloride (Fluka, 98%), Nickel (II) protoporphyrin IX chloride (Frontier Science), Copper (II) protoporphyrin IX chloride (Frontier Science), Rhodium (II) protoporphyrin IX chloride (Frontier Science) were used as received without further purification. All other chemicals were p.a. grade. Electrolyte solutions of pH 1, 2 and 3 were made of 0.1 M $HClO_4$ (Merck, 70%), 90 mM $NaClO_4$ (Sigma-Aldrich, $\geqslant$ 98.0%) with 10 mM $HClO_4$ and 99 mM $NaClO_4$ with 1 mM $HClO_4$, respectively. 0.1 M $NaNO_3$ (Merck, 99.99%) /$LiNO_3$ (Brunschwig chemie, 99.999%) was added for the nitrate reduction experiments and 4 mM $NaNO_2$ (Sigma-Aldrich, 99.999%) for the nitrite reduction experiments. Water was purified through a Milli-Q Plus Ultra-pure water systerm (Millipore Co.). Resistivity of the purified water was greater than 18.2 MΩ·cm. Pyrolytic graphite (Carbone-Lorraine) was fabricated into a home-made disc electrode with a diameter of 5 mm.

4.2.2. Electrochemistry

All glassware was boiled in a mixture of concentrated sulfuric acid and nitric acid, and subsequently boiled in Milli-Q water 5 times before all experiments. Electrolyte solutions were purged with Ar (purity grade 6.0, Hoekloos) for 15 minutes before measurement to remove dissolved oxygen. Either an Autolab PGSTAT20 (bi)potentiostat or an Ivium potentiosat was used for the cyclic voltammetry experiments. Electrochemical experiments were conducted in a home-made one-compartment three-electrode cell: the working electrode was a metal protoporphyrin immobilized pyrolytic graphite electrode; the counter electrode was a platinum wire; the reference electrode was a reversible hydrogen electrode (RHE), all potentials in this paper are referred to this electrode. The electrochemical reduction of nitrate/nitrite experiments were also conducted on blank pyrolytic graphite electrode, which showed no activity indicating that Platinum counter electrode did not interfere with the reaction.

The metalloprotoporphyrin solutions and the metalloprotoporphyrin immobilized PG electrode were prepared as in our previous work[27]. 1.6 mg of the particular metalloprotoporphyrin was dissolved in 5 ml of a 0.01 M borate solution (pH=10) to make a 0.5 mM metalloprotoporphyrin solution. The PG electrode was abraded using P500 and P1000 SiC sandpaper and ultrasonicated in MilliQ water for 1 min, after which it was dried using compressed air. The saturation of porphyrin on the electrode surface was done by dipping the electrode into certain metalloprotoporphyrin solution for 5 min. Before transferring to the electrochemical cell, the electrode was rinsed with MilliQ water.

Cyclic voltammetry (CV) was utilized to ascertain successful immobilization of metal-protoporphyrins (data not shown here). As in our prior work[27], a redox peak representing the Co^{III}/Co^{II} or Fe^{III}/Fe^{II} couple was observed around 0.82 V and 0.08 V, respectively. The Rh^{II}/Rh^{I} redox couple showed a peak around 0.2 V, while Ni^{II} and Cu^{II} protoporphyrins showed no peak in the potential range we studied. After the electrochemical reduction of nitrate, the presence of the Co^{III}/Co^{II} redox couple was checked again using cyclic voltammetry to investigate the stability of the catalyst. The

redox peak of the cobalt couple was still observed at pH 3, despite a lower current density, but no peak could be resolved at pH 1 due to a substantially higher background current. However, pre- and post-electrolysis inspection by means of ex situ XPS of the CoPP modified PG electrode before and after a 1 hour electrolysis experiment at -0.8 V showed no change in the cobalt oxidation state[28]. This suggests that at pH=1 the surface termination of the pyrolytic graphite changes significantly during the polarization to very negative potential, but that the Cobalt porphyrin is stable on this time scale.

4.2.3. On-line electrochemical mass spectroscopy (OLEMS)

The online electrochemical mass spectrometry (OLEMS) setup, which was used to detect the volatile products during cyclic voltammetry, consisted of an Evolution mass spectrometry system (European Spectrometry Systems Ltd)[29]. A PEEK tip with inner diameter of 0.51 mm, which contained a porous Teflon plug, was placed close (~10 μm) to the electrode surface. All the gas products were collected through a PEEK capillary (connected to the tip) leading to the mass spectrometer chamber, in which the pressure was kept below 10^{-6} mbar. A 2400 V SEM voltage was used except for hydrogen (m/z=2), for which the voltage was 1500 V. The tip was cleaned prior experiments by dipping into a solution of 0.2 M $K_2Cr_2O_7$ in 2 M H_2SO_4 for 15 minute and rinsing with MilliQ water thoroughly. The products were detected while the cyclic voltammogram was taken in the potential range from 0 V to -1.5 V by an Ivium A06075 potentiostat with the scan rate of 1 mVs^{-1}.

4.2.4. On-line ion chromatograpy (IC)

The online ion chromatography (IC) experiments were conducted as in our previous work[30]. The samples were collected every minute using an automatic fraction collector (FRC-10A, Schimadzu) by positioning a Teflon tip close to the middle of working electrode while a linear voltammogram was taken by an Autolab potentiostat (Pgstat20) in a range from 0 V to -1.5 V at a scan rate of 1 mVs^{-1}. The waiting time at the initial potential (0 V) has no influence on the products formed. A microtiter plate with collected samples was placed onto the autosampler (SIL-20A) holder of an ion chromatography unit

(Schimadzu, Prominence) with a conductivity detector (CCD-10Ap, Schimadzu). Samples with a volume of 20 μL were injected into and analyzed through two series of Shodex IC Y-521 columns, of which the temperature was set to 30 ºC, to monitor NH_4^+ and NH_3OH^+ cations. A 2.5 mM nitric acid solution (Merck, Suprapur, 65%) was used as eluent at a flow rate of 8 $mLmin^{-1}$. $LiNO_3$ and $NaNO_2$ were used as substrates for nitrate and nitrite reduction respectively. The concentration of $LiNO_3$ was 0.1 M. As $LiNO_2$ was unstable and a high concentration of sodium cation will overlap with the signal of NH_4^+ and NH_3OH^+, the concentration of $NaNO_2$ was 4 mM.

4.3. Results and Discussion

The catalytic activity of the PG electrode modified with five different metal-center protoporphyrins for the electrochemical reduction of nitrate has been investigated using online ion chromatography in 0.1 M $LiNO_3$ solution at pH 1. Figure 1(a) and 1(b) show the ammonium (NH_4^+) and hydroxylammonium (NH_3OH^+) formation respectively, with metal centers iron (Fe), cobalt (Co), nickel (Ni), copper (Cu) and rhodium (Rh). All metal protoporphyrins show similar trends in the formation of products except for iron which shows a significant increase in the formation of NH_4^+ and NH_3OH^+ from a potential more negative than -1.17 V. The concentration of NH_3OH^+ produced at all catalysts, except for iron protoporphyrin, is from 0.5 mM to 1 mM at the most negative potential, which is always higher than that of NH_4^+, which is below 0.5 mM. Figure 1(c) shows a plot of the NH_3OH^+ selectivity of all catalysts, which is defined as the ratio between the concentration of NH_3OH^+ and the sum of the concentration of NH_3OH^+ and NH_4^+. Cobalt protoporphyrin (CoPP) shows the highest selectivity towards NH_3OH^+ in the whole potential range. NH_3OH^+ is the only product from -0.44 V to -0.81 V, with the selectivity decreasing at more negative potentials but still NH_3OH^+ remains the dominant product. We note that the selectivity as shown in Fig.1c is sensitively dependent on the exact experimental conditions (i.e voltammetric sweep rate and sample collection frequency). Electrolysis experiments at fixed conditions yield NH_4^+ at lower potential (see below). Therefore, the value of Fig.1c is primarily qualitative, and leads to the conclusion that the superior selectivity of CoPP

toward NH_3OH^+ makes it the most interesting catalyst. Therefore we focused on this system in the rest of our studies.

The cyclic voltammograms (CVs) measured during the electrochemical reduction of nitrate at a CoPP modified PG electrode at pH 1 and pH 3 are reported in Figure 2 along with the CVs for hydrogen evolution reaction (HER) for comparison. At pH 1, the absolute peak current density for HER at -1.5 V is almost 2 times higher than that in the presence of nitrate, which means that nitrate, or intermediates formed during its electrochemical reduction, substantially suppresses the hydrogen evolution reaction. Therefore there must be a competition between protons and nitrate for the active site of the cobalt protoporphyrin. The electrochemical nitrate reduction leads to a reduction wave at potentials between ca. -0.5 and -1.5 V, in agreement with the formation of NH_3OH^+ and NH_4^+ in this potential window in Figure 1. Despite the suppression of the hydrogen evolution reaction, H_2 is still produced, as we will show further below using OLEMS. The reduction wave for nitrate reduction disappears almost completely when the pH is increased to 3. This agrees with our previous general observation that a high concentration of protons enhances the electrochemical reduction of nitrate[31]. Remarkably, the absolute current density for the HER at -1.5 V, which is about 10 mA/cm^2, is now lower than that of electrochemical reduction of nitrate, which is about 15 mA/cm^2. This suggests a pH-dependent competition between the reduction of nitrate, protons and water (which at pH=3 is probably the main contributor to the HER, in contrast to pH=1). Also, results to be presented below suggest that N_2O and N_2 are more important products of nitrate reduction at pH=3 than hydroxylamine and ammonia.

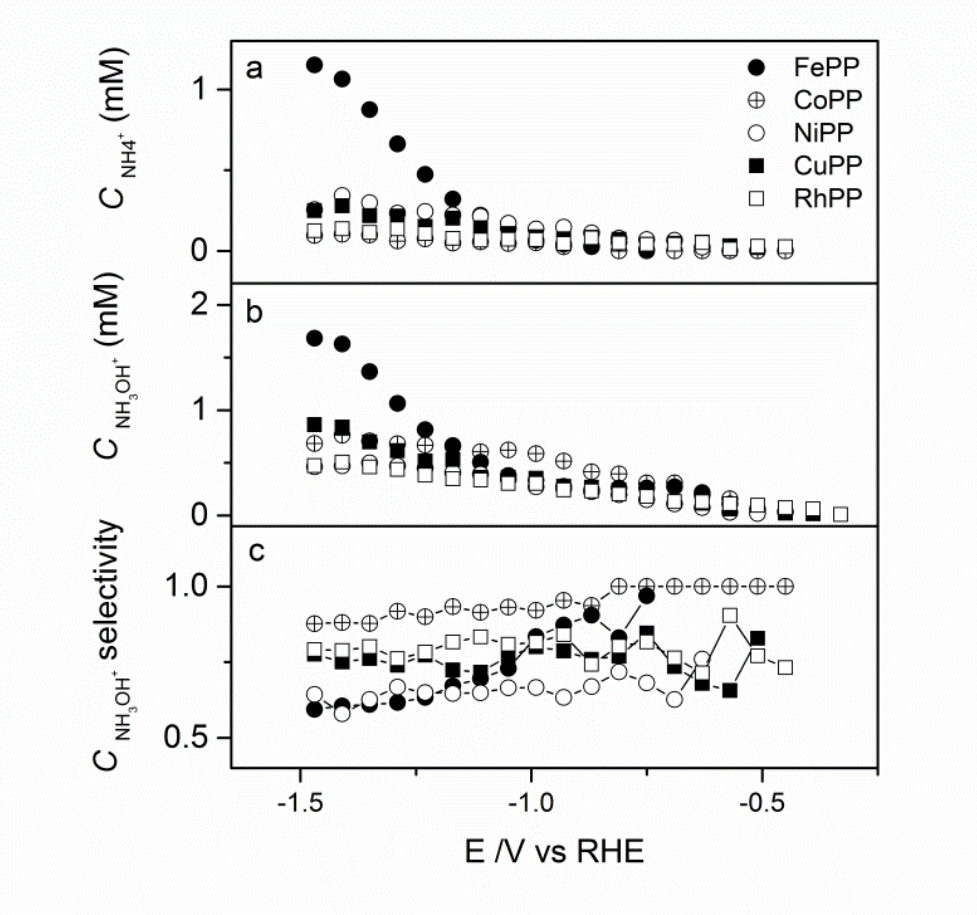

Figure 1. Nitrate reduction on different metal-center protoporphyrins at pH 1, concentration of products obtained while conducting linear sweep voltammetry (LSV) at a scan rate of 1 mVs^{-1} from 0 V to -1.5 V in combination with online ion chromatography (IC). (a) NH_4^+ concentration vs potential on Iron protoporphyrin (FePP), Cobalt protoporphyrin (CoPP), Nickel protoporphyrin (NiPP), Copper protoporphyrin (CuPP), and Rhodium protoporphyrin (RhPP); (b) NH_3OH^+ concentration vs potential on different metal-center protoporphyrins; (c) the ratio of the concentration of NH_3OH^+ to the sum of the concentration of NH_3OH^+ and NH_4^+.

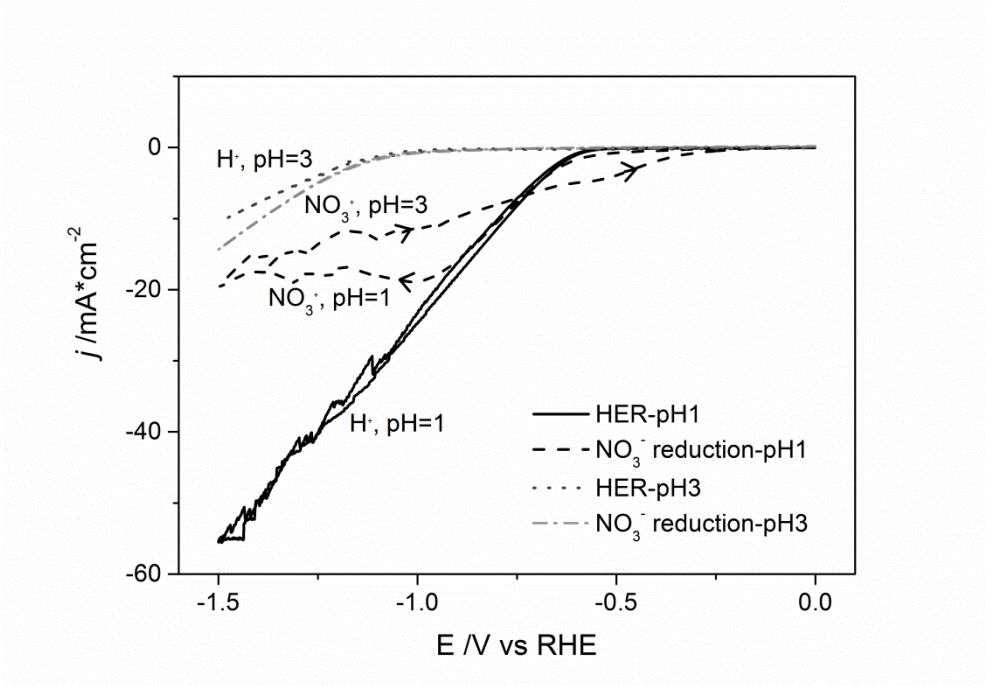

Figure 2. Influence of pH on the cyclic voltammetry profiles of nitrate reduction (0.1 M $NaNO_3$) and hydrogen evolution reaction (HER) on cobalt protoporphyrin immobilized PG electrode in 0.1 M perchlorate solution (pH =1 and 3), scan rate is 100 mV s^{-1}.

Figure 3 presents the plots of the concentration of NH_4^+ and NH_3OH^+ produced from electrochemical nitrate reduction by the immobilized CoPP as a function of potential at pH 1 and pH 2. Figure 3(a) shows that NH_4^+ is formed at an almost equal concentration at pH 1 and pH 2, with a slightly higher concentration for pH 2. The same experiment was conducted at pH 3, but no NH_4^+ was detected (result not shown here). Figure 3(b) shows that NH_3OH^+ is formed earlier than NH_4^+ regardless of pH, from around -0.5 V. At pH 1, NH_3OH^+ increases with potential until to -1.0 V where it reaches its maximum concentration and remains constant until the most negative potential, although with some fluctuation. However, the concentration of NH_3OH^+ is dramatically decreased with the pH increased to 2. The same experiment was also conducted at pH 3 and no NH_3OH^+ was detected. The significant conclusion of Figure 3 is that pH has a very substantial influence on the selective formation of NH_3OH^+. With a small pH increase from 1 to 2, the formation

of NH_3OH^+ is almost completely suppressed, whereas the production of NH_4^+ remains constant. At pH 3, neither NH_4^+ nor NH_3OH^+ is observed.

It is generally accepted that the difficult step in nitrate reduction is its conversion to nitrite[5]. It is therefore worthwhile to study the electrochemical reduction of nitrite under the same conditions as nitrate reduction. Figure 4 shows the formation of NH_3OH^+ and NH_4^+ from nitrite reduction on the CoPP immobilized PG electrode at different pH. It is important to keep in mind that the concentration of nitrite is only 4 mM which is 25 times smaller than the concentration of nitrate. The fact that the measured concentrations in Figure 4 are similar to Figure 3 shows that nitrite is indeed significantly more reactive than nitrate. Figure 4(a) shows the NH_4^+ formation at different pH. With a pH increase from 1 to 2, the concentration of NH_4^+ is slightly higher, which is similar to the case of nitrate reduction. There is still NH_4^+ produced at pH 3, only the amount is significantly less than that at pH 2. Figure 4(b) shows that the formation of NH_3OH^+ exhibits the same trend with pH as nitrate reduction, in the sense that the formation of NH_3OH^+ is dramatically suppressed with higher pH. The inserted plot in Figure 4(b) zooms in at the formation of NH_3OH^+ at pH 2 and 3, showing that NH_3OH^+ was barely produced at pH 3. Despite the small amount of NH_4^+ formed from nitrite reduction at pH 3, the electrochemical reduction of nitrate and nitrite exhibit the same selectivity and pH sensitivity, from which we can deduce that the electrochemical reduction of nitrate indeed goes through nitrite as intermediate.

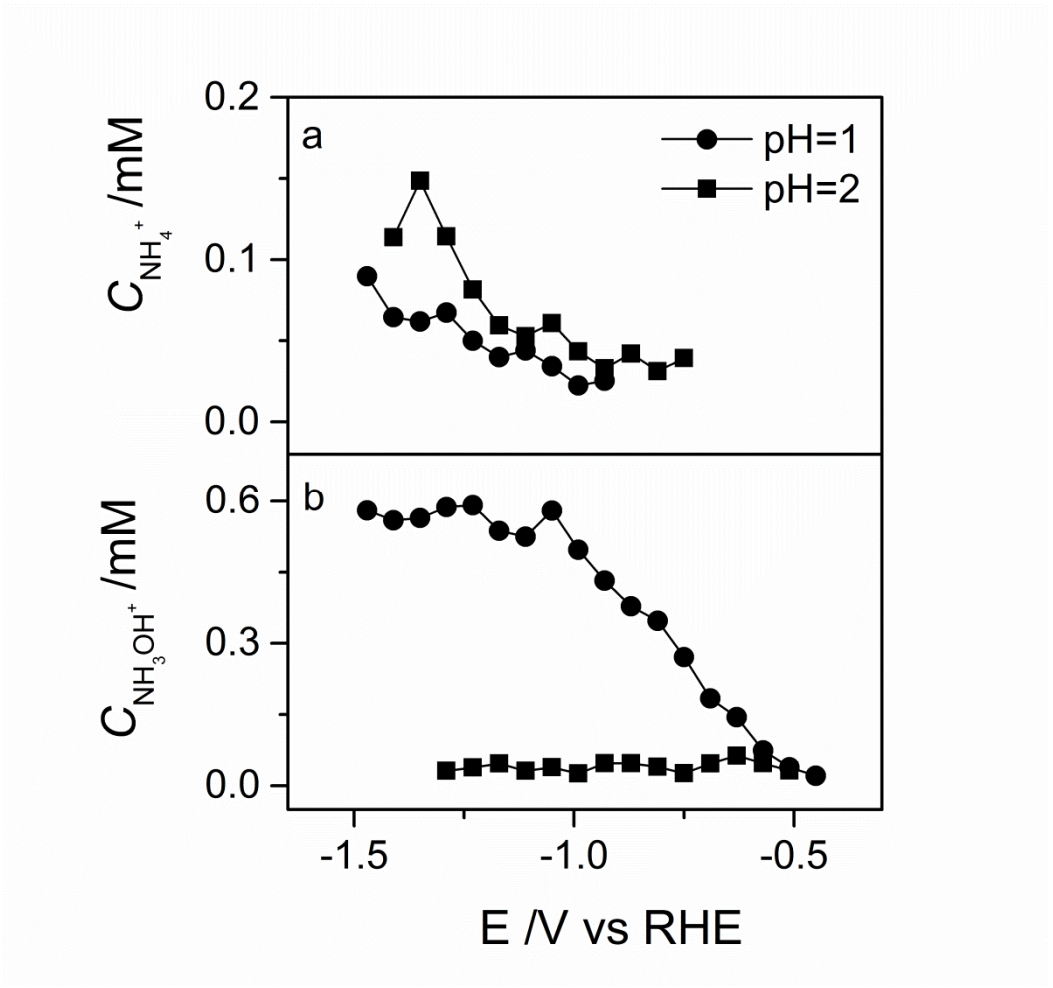

Figure 3. Nitrate electrochemical reduction on cobalt protoporphyrin immobilized PG electrode at pH=1 (0.1 M $HClO_4$) and pH=2 (10 mM $HClO_4$ + 90 mM $LiClO_4$). (a) the concentration of NH_4^+ as a function of potential; (b) the concentration of NH_3OH^+ as a function of potential, 0.1 M $LiNO_3$. Scan rate is 1 mV s^{-1}.

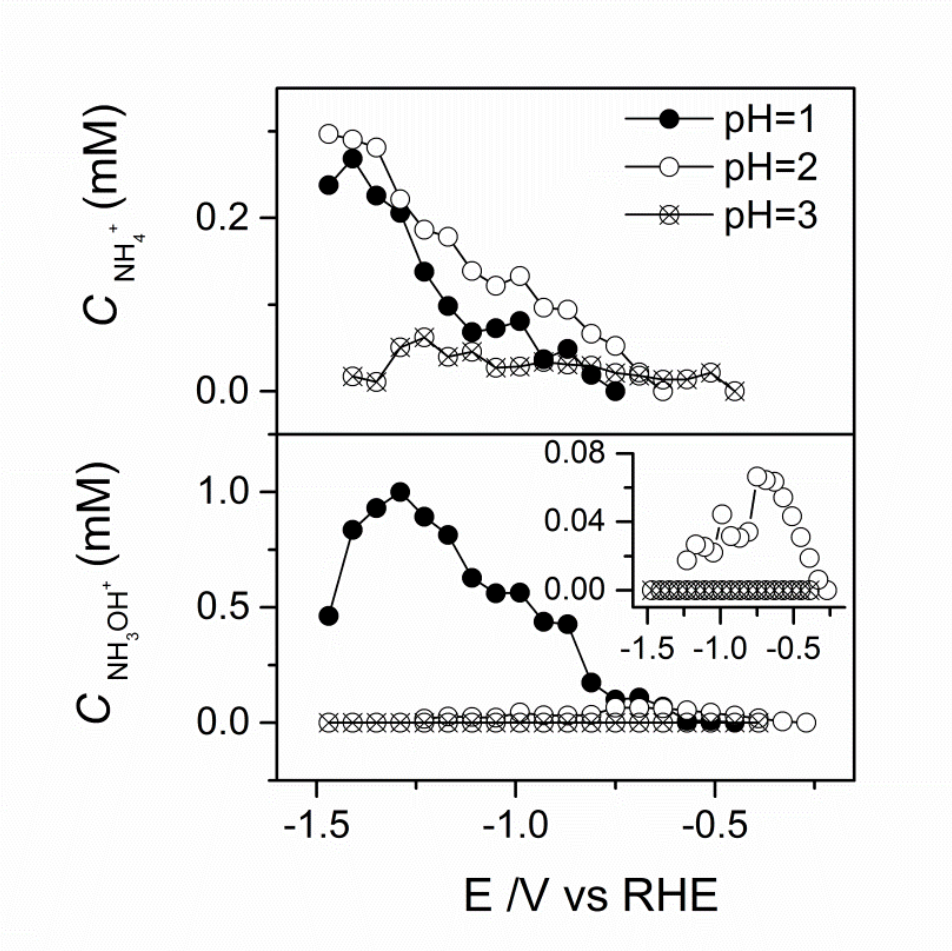

Figure 4. Nitrite electrochemical reduction on cobalt protoporphyrin immobilized PG electrode at pH=1 (0.1 M $HClO_4$), pH=2 (90 mM $NaClO_4$ + 10 mM $HClO_4$) and pH=3 (99 mM $NaClO_4$ + 1 mM $HClO_4$). (a) meausred NH_4^+ concentration vs potential; (b) measured NH_3OH^+ concentration vs potential, 4 mM $NaNO_2$. Scan rate is 1 mV s^{-1}.

NO is considered as the nitrite-derived substrate in acid media as there is a homogeneous-phase decomposition reaction of HNO_2 to NO for pH<5[26, 32]. It is therefore important to investigate the formation of NO at different pH on the immobilized cobalt protoporphyrin. Figure 5(d-f) shows the formation of NO at pH 1 to 3 detected by OLEMS during the electrochemical reduction of nitrate. It should be pointed out that the m/z=30 signal was not corrected for the N_2O fragmentation. Figure 5(d) shows the variation of NO

vs potential at pH 1, from which it is observed that NO forms at the beginning of the reaction (i.e. at positive potentials, when the electrochemical current is still very low) and is also formed when the voltammetry scans back in the positive direction. Figure 5(e) shows the same trend as Figure 5(d), but the intensity of the NO ionic current at pH 2 is 40 times lower than that at pH 1. We also find that a small amount of NO is produced at very negative potential, which we ascribe to the fragment of the N_2O detected as the by-product of the nitrate reduction, as will be discussed later. At pH 3, there is no NO detected at neither the beginning of the reaction nor the end of the back scan in Figure 5(f), which may indicate that NO is not produced from nitrate/nitrite at this pH. A small amount of NO was measured from -1.0 V to -1.5 V, which may come from the fragment of N_2O (see below). These results are in full agreement with our previous conclusion that the main source of NO is the pH-dependent decomposition reaction of HNO_2 in solution[27].

Other possible volatile products of electrochemical nitrate reduction were monitored using OLEMS at different pH, as is shown in Figure 5 (g-o). The N_2O formation exhibits a large difference between pH 1 and 2, 3 as shown in Figure 5(g) to Figure 5(i). At pH 1, N_2O is produced at the beginning of the electrochemical reduction of nitrate and the ion current decreases at around -0.4 V. As the potential goes to more negative potential, N_2O is observed again at -1.0 V. When cyclic voltammetry scans back toward positive direction, N_2O is formed again at -0.35 V. At pH 1, the formation of N_2O shows trends very similar to NO apart from the small amount of N_2O formation at very negative potential. However, N_2O is not formed neither at the beginning nor at the end of the back scan at pH 2 and 3, instead it is only observed at potentials below -1.0 V in a very small amount. Fragments m/z = 28 and m/z = 2, assigned to N_2 and H_2 respectively, are detected at pH 1 to 3 as shown Figure 5(j-o). The formation of N_2 and H_2 displays similar trends at different pH, as both are formed at relatively negative potential starting from -1.0 V. The exception is at pH 1 for which H_2 and N_2 evolution start earlier around -0.5 V. The ion current corresponding to H_2 shows a peak at ca. -1.0 V. Compared with results from the cyclic voltammograms at pH 1, the formation of H_2 is suppressed when the electrochemical reduction of nitrate reaches a plateau value.

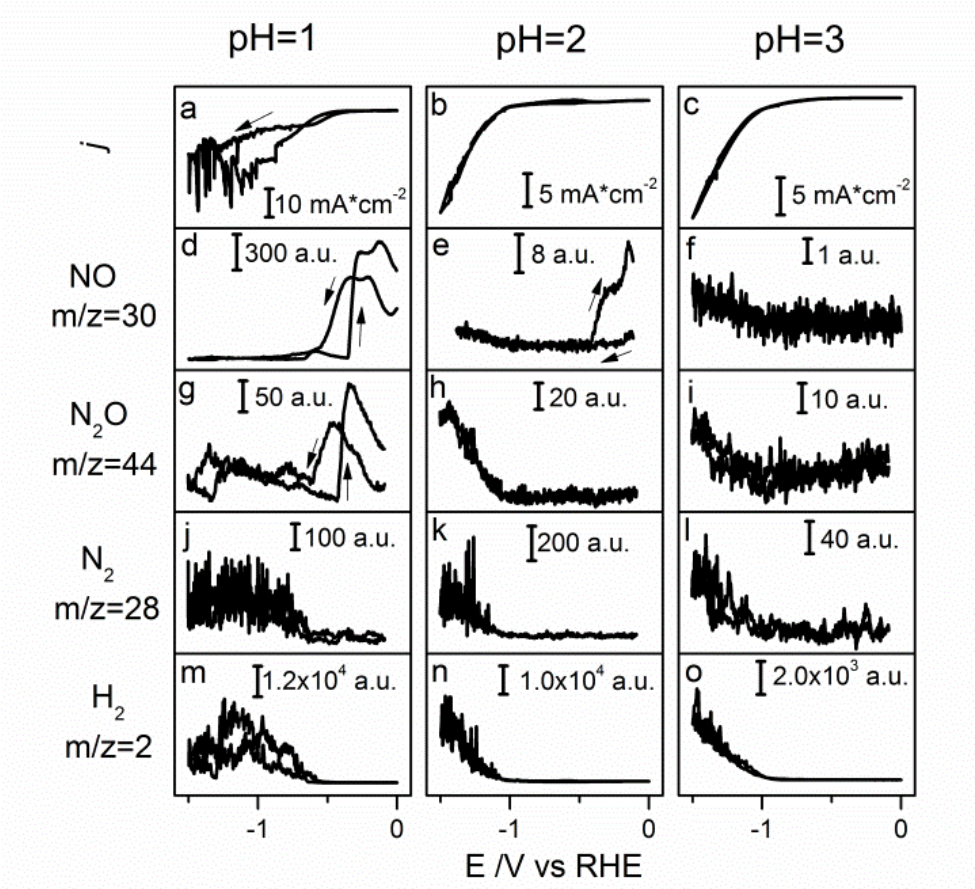

Figure 5. Volatile products detected by online electrochemical mass spectroscopy (OLEMS) during electrochemical nitrate reduction on cobalt protoporphyrin immobilized PG electrode in 0.1 M $NaNO_3$ at different pH. Rows show NO, N_2O, N_2 and H_2 formation respectively; First column: pH 1, 0.1 M $HClO_4$ solution; Second column: pH 2, 10 mM $HClO_4$ + 90 mM $NaClO_4$; and Third column: pH 3, 1 mM $HClO_4$ + 99 mM $NaClO_4$. Scan rate 1 mV s^{-1}.

Figure 6 shows the local concentrations of NH_3OH^+ and NH_4^+ formed from the electrochemical reduction of hydroxylamine verified vs potential at different pH. At pH 1, no NH_4^+ formed from hydroxylamine reduction. NH_4^+ is produced as the pH is increased to 2, and simultaneous with NH_4^+ formation, there is a decrease of hydroxylamine concentration. At pH 3, the concentration of NH_4^+ produced is higher than that at pH 2.

However, when the potential sweeps to potentials more negative than -1.25 V, the concentration of NH_4^+ begins to decline, while hydroxylamine concentration also diminishes. Comparing to Figure 2, this potential corresponds to the onset of H_2 evolution, which may perhaps lead to a local mixing and a lower local concentration of the NH_4^+ in the collected samples.

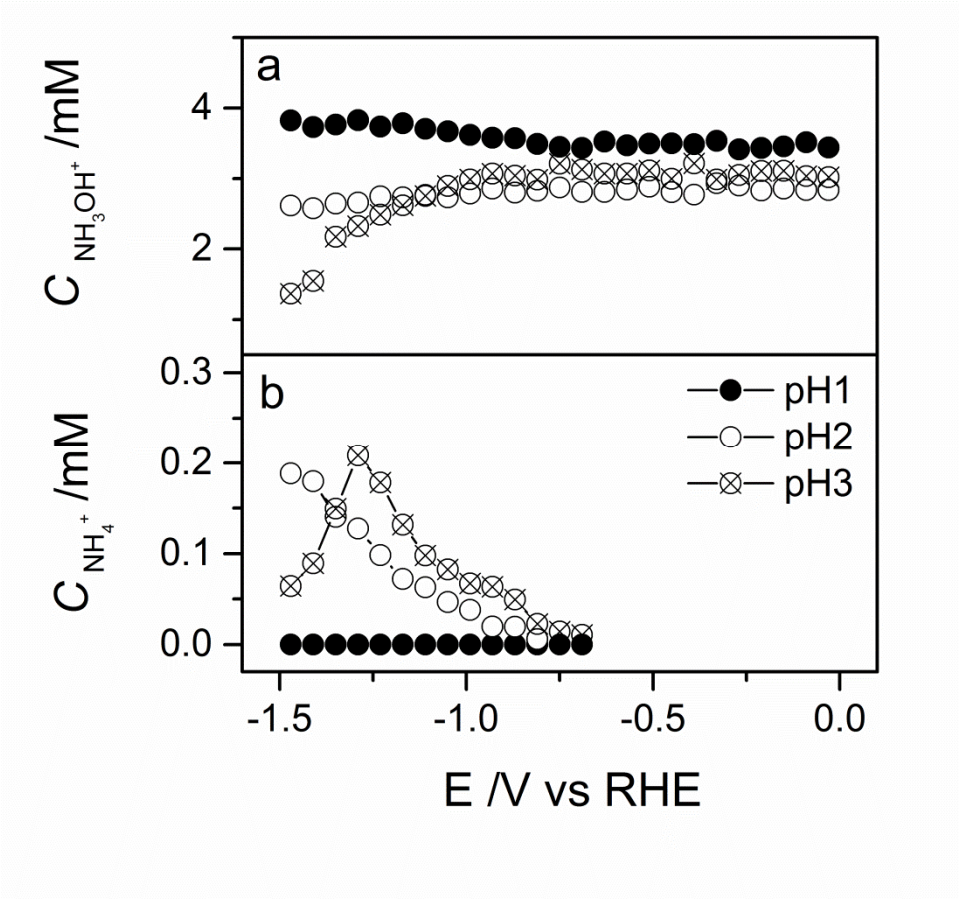

Figure 6. Electrochemical reduction of hydroxylamine on cobalt protoporphyrin immobilized PG electrode from pH 1 to 3. (a) the profiles of NH_3OH^+ concentration vs potential; (b) the profiles of NH_4^+ concentration vs potential. Scan rate is 1 mV s^{-1}. Solution concentration of hydroxylamine is 4 mM.

Finally, a potential controlled electrolysis was conducted for 2 hours to investigate the stability of cobalt protoporphyrin and the formation of NH_3OH^+ and NH_4^+. Figure 7 shows the plots of ion chromatography analysis of samples collected from long-term electrolysis of nitrate reduction in 0.1 M $LiNO_3$ at pH 1. Figure 7(a) shows that at a potential of -0.5 V, NH_3OH^+ is the only product, albeit in a relatively small amount. Up to 1 hour, NH_3OH^+ is stably produced despite some fluctuations from the sample collection. After 1 hour, the concentration gradually decreases, reaching 0.05 mM at the end of the electrolysis. Figure 7(b) displays the electrolysis results at -0.75 V. At this potential both NH_4^+ and NH_3OH^+ are produced and their amounts are dramatically increased compared to -0.5 V. The concentrations of NH_4^+ and NH_3OH^+ first increase to reach a maximum value at ca. 30 minutes after which they decrease to a steady state. Note that the concentration of NH_4^+ obtained in this experiment is considerably higher than in Figure 1, due to the different experimental conditions (i.e. longer electrolysis time at fixed potential).

Based on the results discussed above, we can formulate a tentative mechanism for the nitrate electroreduction catalyzed by cobalt protoporphyrin immobilized pyrolytic graphite electrode. In agreement with our previous work[31], nitrate electroreduction is highly pH dependent. The rate-determining step is the conversion of nitrate to nitrite, given by the following proton-coupled electron transfer reaction:

$$NO_3^- + 2H^+ + 2e^- \rightarrow NO_2^- + H_2O \quad (1)$$

Yang et al.[31] found that equation (1) is enhanced at low pH, suggesting that HNO_3 is the actual reducible species. The selectivity of the overall nitrate reduction then depends on the consecutive reduction of NO_2^-. However, in acidic solution (pH < 5) , Duca et al.[26] found that NO formed from a homogeneous decomposition reaction of HNO_2 is the main reactant on iron-based protoporphyrin, as opposed to the direct electrochemical reduction of NO_2^-:

$$NO_2^- + H^+ \leftrightarrow HNO_2 \quad (2)$$

$$2HNO_2 \leftrightarrow NO + NO_2 + H_2O \quad (3)$$

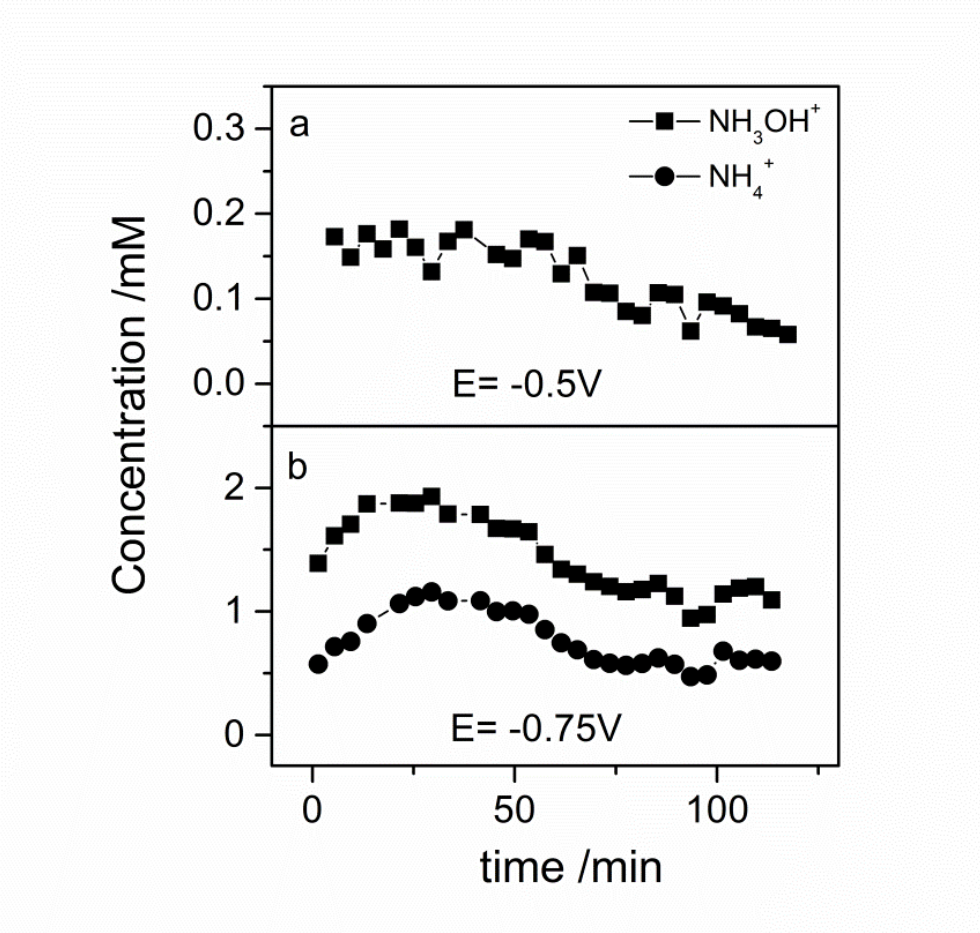

Figure 7. Concentrations of NH_3OH^+ and NH_4^+ as determined by online ion chromatography during a 2 hours potential controlled electrolysis of nitrate reduction (0.1M $LiNO_3$) at pH=1 (0.1M $HClO_4$). (a) E = -0.5 V; (b) E = -0.75 V.

The NO adduct formed through equation (4) was confirmed using spectroscopic studies by Cheung et al.[13] and Ma et al.[18]. The most stable NO adducts formed were $[Co^{II}(2\text{-}TMPyP)(NO)]^{4+}$ and $Fe^{II}(NO)PP$, which indicates that the M^{II} oxidation state is not the oxidation state catalyzing NO reduction. The NO adduct was reduced to M-HNO by a simultaneous one-proton, one-electron transfer as shown below in equation (5)[25,26], which is

the precursor to different gas and non-volatile products. The gaseous product N_2O is formed by the reaction of M-HNO adduct with the NO in the solution, a reaction whose mechanism on iron-based porphyrins has been studied in detail in our earlier work.[25,26] The overall reaction for the formation of N_2O is shown in equation (6) below. N_2O will consecutively react to N_2, but this reaction is very slow. We assume this reaction to be the source of N_2 formation in Figure 5. In Figure 5, there is a second pathway leading to the formation of N_2O at potentials below ca. -1 V (vs. RHE) which appears as distinct from the N_2O formation at higher potentials. The most likely source of N_2O at these very negative potentials is the homogeneous reaction between nitrite and hydroxylamine[5].

$$M + NO \rightarrow M\text{-}NO \quad (4)$$

$$M\text{-}NO + e^- + H^+ \rightarrow M\text{-}HNO \quad (5)$$

$$M\text{-}HNO + NO + H^+ + e^- \rightarrow M + N_2O + H_2O \quad (6)$$

The main non-volatile products are hydroxylamine and ammonia, which we speculate to be formed either through a sequential pathway or a parallel pathway. For the sequential pathway, the further reduction reaction of M-HNO leads to the formation of hydroxylamine through equation (7).

$$M\text{-}HNO + 2H^+ + 2e^- \rightarrow M + NH_2OH \quad (7)$$

Ammonia is then formed through the sequential reduction of hydroxylamine, as presented in Figure 6(b) for pH 2 and 3. We further speculate that the pH dependent selectivity in such a sequential reaction could depend on the protonation state of the hydroxylamine, i.e. NH_3OH^+ vs. NH_2OH, with the ratio of the concentrations between NH_3OH^+ and NH_2OH being strongly influenced by the pH as the corresponding pKa is 5.9. The results of hydroxylamine reduction confirm that NH_2OH is the actual precursor for the formation of ammonia, explaining why hydroxylamine reduction shows a higher activity at

pH 3. We suspect that there should be an optimal pH for the hydroxylamine reduction, which needs further investigation.

Figure 6 shows that hydroxylamine cannot be reduced to ammonia at pH 1, but the electrochemical reduction of nitrate does produce ammonia at pH 1 as presented in Figure 4. This suggests that the formation of hydroxylamine and ammonia may also follow a parallel pathway, with the HNO adduct being the precursor to both hydroxylamine and ammonia formation. In this case, the pH dependent electrochemical reactivity of M-HNO would determine the final product.

In our previous work, immobilized hemin (FePP) was used to catalyze the electrochemical reduction of NO and nitrite[25,26]. The main product at low pH was hydroxylamine with a small amount of N_2O. A possible explanation for the discrepancy with the results reported here is the different working potential window. In the former work, the most negative potential was -0.5 V, since both NO and nitrite are highly reactive at low pH, in contrast to the potential window of -0.5 to -1.5 V used here, due to the fact that nitrate is much less reactive. From the long-term electrolysis experiments reported here, hydroxylamine is the only product at the least negative potential -0.5 V, which is consistent with the previous study. Under more reductive conditions (i.e. more negative potentials), ammonia is also formed. Moreover, the formation of ammonia is time dependent, as can be concluded from the comparison of Figures 1 and 7. Longer electrolysis times at fixed potential (Figure 7) yield more ammonia than during linear sweep voltammetry (Figure1). We consider these observations further arguments in favor of the sequential pathway.

4.4. Conclusions

We have shown that adsorbed metal protoporphyrins can reduce nitrate to NH_2OH/NH_3OH^+ and NH_3/NH_4^+ in acid media at sufficiently negative potentials, from ca. -0.5 V (vs. RHE). At less negative potentials, NO and N_2O are formed, with a very small amount of N_2. Among all different metal centers, the cobalt protoporphyrin shows highest selectivity towards NH_2OH/NH_3OH^+. The mechanism of the reaction has been studied using voltammetry and online mass spectrometric and ion chromatographic methods.

Importantly, pH affects almost every step of the reaction, leading to a pH dependent product selectivity. Low pH (~1) enhances the rate-determining conversion of nitrate to nitrite and leads to a more selective formation of hydroxylamine. Slightly higher pH (2-3) lowers the overall reactivity and shifts selectivity to ammonia. The most likely explanation for this intricate pH dependence is a sequential pathway in which hydroxylamine is an intermediate in the formation of ammonia.

4.5. Acknowledgments

J.S. acknowledges the award of a grant of the Chinese Scholarship Council (CSC).

REFERENCES

1. Averill, B. A. Dissimilatory Nitrite and Nitric Oxide Reductases. *Chem. Rev.* **1996**, 96 (7), 2951-2964.

2. Spalding, R. F.; Exner, M. E. Occurrence of Nitrate in Groundwater—A Review. *J. Environ. Qual.* **1993**, 22 (3), 392-402.

3. Nolan, B. T.; Ruddy, B. C.; Hitt, K. J.; Helsel, D. R. Risk of Nitrate in Groundwaters of the United StatesA National Perspective. *Environ. Sci. Technol.* **1997**, 31 (8), 2229-2236.

4. Li, M.; Feng, C.; Zhang, Z.; Sugiura, N. Efficient electrochemical reduction of nitrate to nitrogen using Ti/IrO_2–Pt anode and different cathodes. *Electrochim. Acta* **2009**, 54 (20), 4600-4606.

5. Rosca, V.; Duca, M.; de Groot, M. T.; Koper, M. T. M. Nitrogen Cycle Electrocatalysis. *Chem. Rev.* **2009**, 109 (6), 2209-2244.

6. Hajipour, A. R.; Mohammadpoor-baltork, I.; Nikbaghat, K.; Imanzadeh, G. Solid-Phase Synthesis of Oximes. *Synth. Commun.* **1999**, 29 (10), 1697-1701.

7. da Cunha, M. C. P. M.; De Souza, J. P. I.; Nart, F. C. Reaction Pathways for Reduction of Nitrate Ions on Platinum, Rhodium, and Platinum−Rhodium Alloy Electrodes. *Langmuir* **2000**, 16 (2), 771-777.

8. Gauthard, F.; Epron, F.; Barbier, J. Palladium and platinum-based catalysts in the catalytic reduction of nitrate in water: effect of copper, silver, or gold addition. *J. Catal.* **2003**, 220 (1), 182-191.

9. Pronkin, S. N.; Simonov, P. A.; Zaikovskii, V. I.; Savinova, E. R. Model Pd-based bimetallic supported catalysts for nitrate electroreduction. *J. Mol. Catal. A: Chem.* **2007**, 265 (1–2), 141-147.

10. Santos, A. L.; Jay Deiner, L.; Varela, H. The effect of ultra-low proton concentration on the electrocatalytic reduction of nitrate over platinum. *Catal. Commun.* **2008**, 9 (2), 269-272.

11. Choi, I. K.; Liu, Y.; Feng, D.; Paeng, K. J.; Ryan, M. D. Electrochemical and spectroscopic studies of iron porphyrin nitrosyls and their reduction products. *Inorg. Chem.* **1991**, 30 (8), 1832-1839.

12. Barley, M. H.; Meyer, T. J. Electrocatalytic reduction of nitrite to ammonia based on a water-soluble iron porphyrin. *J. Am. Chem. Soc.* **1986**, 108 (19), 5876-5885.

13. Cheng, S.-H.; Su, Y. O. Electrocatalysis of Nitric Oxide Reduction by Water-Soluble Cobalt Porphyrin. Spectral and Electrochemical Studies. *Inorg. Chem.* **1994**, 33 (25), 5847-5854.

14. Taniguchi, L.; Nakashima, N.; Yasukouchi, K. Reduction of nitrate to give hydroxylamine at a mercury electrode using cobalt(III)-and nickel(II)-cyclams as catalysts. *Chem. Commun.* **1986**, (24), 1814-1815.

15. Taniguchi, I.; Nakashima, N.; Matsushita, K.; Yasukouchi, K. Electrocatalytic reduction of nitrate and nitrite to hydroxylamine and ammonia using metal cyclams. *J. Electroanal. Chem. Interfacial electrochem.* **1987**, 224 (1–2), 199-209.

16. Li, H.-L.; Chambers, J. Q.; Hobbs, D. T. Electrocatalytic reduction of nitrate and nitrite at nafionR-coated electrodes in concentrated sodium hydroxide solution. *J. Electroanal. Chem. Interfacial electrochem.* **1988**, 256 (2), 447-453.

17. Ma, L.; Zhang, B.-Y.; Li, H.-L.; Chambers, J. Q. Kinetics of nitrate reduction by cobalt-cyclam incorporated Nafion® redox polymer. *J. Electroanal. Chem.* **1993**, 362 (1–2), 201-205.

18. Ma, L.; Li, H. Electrocatalysis of adsorbed Co-cyclam at Au electrodes for nitrate reduction in concentrated alkaline solution. *Electroanalysis* **1995**, 7 (8), 756-758.

19. Simon, E.; Sablé, E.; Handel, H.; L'Her, M. Electrodes modified by conducting polymers bearing redox sites: Ni- and Co-cyclam complexes on polypyrrole. *Electrochim. Acta* **1999**, 45 (6), 855-863.

20. Li, H. L.; Chambers, J. Q.; Hobbs, D. T. Electroreduction of nitrate ions in concentrated sodium hydroxide solutions at lead, zinc, nickel and phthalocyanine-modified electrodes. *J. Appl. Electrochem.* **1988**, 18 (3), 454-458.

21. Chebotareva, N.; Nyokong, T. Metallophthalocyanine catalysed electroreduction of nitrate and nitrite ions in alkaline media. *J. Appl. Electrochem.* **1997**, 27 (8), 975-981.

22. Kuwabata, S.; Uezumu, S.; Tanaka, K.; Tanaka, T. Reduction of NO_3^- giving NH_3 using a $(Bu_4N)_3[Mo_2Fe_6S_8(SPh)_9]$-modified glassy carbon electrode. *Chem. Commun.* **1986**, (2), 135-136.

23. Keita, B.; Abdeljalil, E.; Nadjo, L.; Contant, R.; Belgiche, R. First examples of efficient participation of selected metal-ion-substituted heteropolyanions in electrocatalytic nitrate reduction. *Electrochem. Commun.* **2001**, 3 (2), 56-62.

24. Zhang, Z.; Qi, Y.; Qin, C.; Li, Y.; Wang, E.; Wang, X.; Su, Z.; Xu, L. Two Multi-Copper-Containing Heteropolyoxotungstates Constructed from the Lacunary Keggin Polyoxoanion and the High-Nuclear Spin Cluster. *Inorg. Chem.* **2007**, 46 (20), 8162-8169.

25. de Groot, M. T.; Merkx, M.; Wonders, A. H.; Koper, M. T. M. Electrochemical Reduction of NO by Hemin Adsorbed at Pyrolitic Graphite. *J. Am. Chem. Soc.* **2005**, 127 (20), 7579-7586.

26. Duca, M.; Khamseh, S.; Lai, S. C. S.; Koper, M. T. M. The Influence of Solution-Phase HNO_2 Decomposition on the Electrocatalytic Nitrite Reduction at a Hemin–Pyrolitic Graphite Electrode. *Langmuir* **2010**, 26 (14), 12418-12424.

27. de Groot, M. T.; Koper, M. T. M. Redox transitions of chromium, manganese, iron, cobalt and nickel protoporphyrins in aqueous solution. *Phys. Chem. Chem. Phys.* **2008**, 10 (7), 1023-1031.

28. Shen J.; Kortlever R.; Kas R.; Birdja Y. Y.; Diaz-Morales O.; Kwon Y.; Ledezma-Yanez I.; Schouten K. J. P.; Mul G.; Koper M.T. M. Electrocatalytic reduction of carbon dioxide to carbon monoxide and methane at an immobilized cobalt protoporphyrin. *Nature Commun.* **2015**, **6**, 8177.

29. Wonders, A. H.; Housmans, T. H. M.; Rosca, V.; Koper, M. T. M. On-line mass spectrometry system for measurements at single-crystal electrodes in hanging meniscus configuration. *J. Appl. Electrochem.* **2006**, 36 (11), 1215-1221.

30. Yang, J.; Kwon, Y.; Duca, M.; Koper, M. T. M. Combining Voltammetry and Ion Chromatography: Application to the Selective Reduction of Nitrate on Pt and PtSn Electrodes. *Anal. Chem.* **2013**, 85 (16), 7645-7649.

31. Yang, J.; Sebastian, P.; Duca, M.; Hoogenboom, T.; Koper, M. T. M. pH dependence of the electroreduction of nitrate on Rh and Pt polycrystalline electrodes. *Chem. Commun.* **2014**, 50 (17), 2148-2151.

32. Park, J. Y.; Lee, Y. N. Solubility and decomposition kinetics of nitrous acid in aqueous solution. *J. Phys. Chem.* **1988**, 92 (22), 6294-6302.